ADVANCES IN ATMOSPHERIC SCIENCES, VOL. 30, NO. 4, 2013, 983–996

Incorporating Groundwater Dynamics and Surface/Subsurface Runoff Mechanisms in Regional Climate Modeling over River Basins in China

QIN Peihua[1] (秦佩华), XIE Zhenghui*[1] (谢正辉), and YUAN Xing[1,2] (袁 星)

[1] *State Key Laboratory of Numerical Modeling for Atmospheric Sciences and Geophysical Fluid Dynamics, Institute of Atmospheric Physics, Chinese Academy of Sciences, Beijing* 100029

[2] *Department of Civil and Environmental Engineering, Princeton University, Princeton, New Jersey* 08544, *USA*

(Received 7 May 2012; revised 11 September 2012; accepted 12 September 2012)

ABSTRACT

To improve the capability of numerical modeling of climate-groundwater interactions, a groundwater component and new surface/subsurface runoff schemes were incorporated into the regional climate model RegCM3, renamed RegCM3_Hydro. 20-year simulations from both models were used to investigate the effects of groundwater dynamics and surface/subsurface runoff parameterizations on regional climate over seven river basins in China. A comparison of results shows that RegCM3_Hydro reduced the positive biases of annual and summer (June, July, August) precipitation over six river basins, while it slightly increased the bias over the Huaihe River Basin in eastern China. RegCM3_Hydro also reduced the cold bias of surface air temperature from RegCM3 across years, especially for the Haihe and the Huaihe river basins, with significant bias reductions of 0.80°C and 0.88°C, respectively. The spatial distribution and seasonal variations of water table depth were also well captured. With the new surface and subsurface runoff schemes, RegCM3_Hydro increased annual surface runoff by 0.11–0.62 mm d^{-1} over the seven basins. Though previous studies found that incorporating a groundwater component tends to increase soil moisture due to the consideration of upward groundwater recharge, our present work shows that the modified runoff schemes cause less infiltration, which outweigh the recharge from groundwater and result in drier soil, and consequently cause less latent heat and more sensible heat over most of the basins.

Key words: groundwater, runoff, river basin, regional climate

Citation: Qin, P. H., Z. H. Xie, and X. Yuan, 2013: Incorporating groundwater dynamics and surface/subsurface runoff mechanisms in regional climate modeling over river basins in China. *Adv. Atmos. Sci.*, **30**(4), 983–996, doi: 10.1007/s00376-012-2095-7.

1. Introduction

Groundwater controls the lower boundary of soil water and surface water controls the upper boundary; both play vital roles in the hydrological cycle. A realistic representation of groundwater and surface water processes in hydrology models and climate models is most important. Several hydrological studies have focused on modeling coupled groundwater and surface water systems (Sophocleous et al., 1999; Sophocleous and Perkins, 2000; Henriksen et al., 2003; Niu et al., 2007; Xie and Yuan, 2010; Di et al., 2011; Xie et al., 2012), static and dynamic water table representation in land surface models (Liang and Xie, 2001; Liang et al., 2003), and climate models (Yuan et al., 2008).

To take into account the effects of surface-groundwater interactions on soil moisture, evapotranspiration, and recharge rate, Liang et al. (2003) developed dynamic groundwater parameters for the three-layer variable infiltration capacity model (VIC-3L) by treating it as a moving-boundary problem, solved by way of the mass-lumped finite element method (Xie

*Corresponding author: XIE Zhenghui，zxie@lasg.iap.ac.cn

et al., 1998, 1999). Yang and Xie (2003) recast the moving-boundary problem as a fixed-boundary problem using a coordinate transformation technique, thereby lowering computation cost. Niu et al. (2007) developed a simple groundwater model (SIMTOP) in which groundwater recharge and discharge processes were represented as a dynamic coupling between the bottom soil layer and an unconfined aquifer. Maxwell and Kollet (2008) used a variably saturated groundwater flow model with integrated overland flow and land surface model processes to examine the interaction of water and energy flow. To investigate the effects of water-table dynamics on regional climate, Yuan et al. (2008) added a transpiration term to Yang and Xie (2003) groundwater model and coupled it into the regional climate model RegCM3 (Pal et al., 2007). Numerical studies of areas affected by the East Asian monsoon throughout one summer season, using RegCM3 coupled with water-table dynamics, showed that the systematic biases of the simulated precipitation were greatly reduced in most areas.

In the present study, the groundwater model developed by Yang and Xie (2003), the surface runoff parameterization developed by Liang and Xie (2001), and a subsurface runoff parameterization (Niu et al., 2005) were integrated into the regional climate model RegCM3. We named the resulting model RegCM3_Hydro. The surface runoff parameterization dynamically incorporated both the Horton and Dunne runoff generation mechanisms within a model grid cell, and also factored in subgrid-scale soil heterogeneity. The upper and lower boundary of the groundwater model were then modified through implementing the surface and subsurface runoff schemes that affect the flux across the surface and base flow in the groundwater model. Two 45-year simulations over the East Asian monsoon area were conducted, using the RegCM3_Hydro model and the original RegCM3 model. And the effects on regional climate of combining groundwater with water-table dynamics and soil moisture were then investigated for seven river basins in China: the Haihe River Basin (HA), Heihe River Basin (HE), Huaihe River Basin (HU), Pearl River Basin (PE), Songhuajiang River Basin (SH), Yellow River Basin (YL), and Yangtze River Basin (YZ).

Section 2 of this paper describes the regional climate model, the groundwater model, the surface/subsurface runoff generation mechanisms, and the structure of the experiment. Section 3 is an evaluation of the model in terms of precipitation, temperature, and the effect of water-table dynamics on the regional climate over the seven studied river basins. Finally, the results of the study are summarized in section 4.

2. Model description and experimental design

2.1 *RegCM3*

The regional climate model used in this study was the International Centre for Theoretical Physics Regional climate model version 3 (RegCM3; Pal et al., 2007); it is an upgraded version of the model originally developed by Giorgi et al. (1993a, b). RegCM3 is a three-dimensional, σ-vertical coordinate, hydrostatic, compressible, primitive-equation model; its dynamical core is based on the hydrostatic version of the fifth-generation Pennsylvania State University/National Center for Atmospheric Research (PSU-NCAR) mesoscale modeling system (MM5, Grell et al., 1994). The key components of RegCM3 are the following:

(1) An atmospheric radiation transfer scheme (Kiehl et al., 1996)

(2) A land surface model (Dickinson et al., 1993; Giorgi et al., 2003)

(3) A planetary boundary layer scheme (Holtslag et al., 1990; Holtslag and Boville, 1993)

(4) An ocean flux parameterization (Zeng et al., 1998)

(5) A resolvable cloud and precipitation scheme (Pal et al., 2000)

Several choices of convective precipitation schemes are embodied in RegCM3. The Grell scheme (Grell, 1993), together with the Fritsch and Chappel closure assumption (Fritsch and Chappell, 1980), were adopted in the present study.

RegCM3 has been used in many studies over areas with spatial resolution from 10 km to 100 km including, among others, regional climate (Gao et al., 2011; Im et al., 2010; Sylla et al., 2010; Thrasher and Sloan, 2010; Gao et al., 2012; Zou and Zhou, 2012), land-atmosphere interaction (Steiner et al., 2005; Van Den Hurk and Van Meijgaard, 2010), data assimilation of soil moisture (Hu et al., 2010), sea-salt radiative effects on regional climate (Zakey et al., 2008), and the effects of El Niño Southern Oscillation (ENSO) and North Atlantic Oscillation (NAO) on storm activity and precipitation (Syed et al., 2010).

2.2 *Groundwater Model*

The groundwater model used in this study is based on the parameterization established by Liang et al. (2003). Let $\alpha(t)$ be the groundwater table depth (L) which represents the distance from the ground surface to water table, and through the coordinate transform (Yang and Xie, 2003), $x = z/\alpha(t), \tau = t$, the groundwater model can then be described as a fixed boundary problem:

$$\begin{cases} \dfrac{\partial\theta}{\partial\tau} - \dfrac{x}{\alpha}\dfrac{d\alpha}{d\tau}\dfrac{\partial\theta}{\partial x} = \dfrac{\partial}{\partial x}\left(\dfrac{D(\theta)}{\alpha^2}\dfrac{\partial\theta}{\partial x} - \dfrac{K(\theta)}{\alpha}\right) - S(z,\tau) , \\ \left[K(\theta) - \dfrac{D(\theta)}{\alpha}\dfrac{\partial\theta}{\partial x}\right]\Big|_{x=0} = q_0(\tau) , \\ \theta(x,\tau)|_{x=1} = \theta_{\rm s} , \\ \theta(x,0) = \theta_0(x), \quad \text{for } 0 \leqslant x \leqslant 1 , \\ \left[K(\theta) - \dfrac{D(\theta)}{\alpha}\dfrac{\partial\theta}{\partial x}\right]\Big|_{x=1} = Q_{\rm b}(\tau) + E_2(\tau) - n_{\rm e}(\tau)\dfrac{d\alpha}{d\tau} , \end{cases} \tag{1}$$

where θ is the volumetric soil moisture content (L^3/L^3); $D(\theta)$ is the hydraulic diffusivity (L^2/T); $K(\theta)$ is the hydraulic conductivity (L/T); $S(z,\tau)$ is the sink item; $q_0(\tau)$ is the flux across the surface (i.e., $z=0$); $\theta_{\rm s}$ is the soil porosity (L^3/L^3); $Q_{\rm b}(\tau)$ is the base flow (L/T); $E_2(\tau)$ is the transpiration from root region in the saturated zone (L/T); and $n_{\rm e}(\tau)$ is the effective porosity of the porous media (L/L). By integrating the transformed Richards equation over $(0,1)$, Eq. (1) can then be numerically solved by the finite element method as described in Liang et al. (2003).

2.3 *Surface and subsurface runoff parameterizations*

In this study, we used the surface runoff parameterization that dynamically represents both the Horton and Dunne runoff generation mechanisms within a model grid cell, together with consideration of the subgrid-scale soil heterogeneity as developed by Liang and Xie (2001), and the subsurface runoff parameterization based on the hydrological model TOPMODEL (Beven and Kirkby, 1979; Sivapalan et al., 1987) developed by Niu et al. (2005). The surface runoff mechanism has been widely used in land surface models (Liang et al., 2003; Tian et al., 2006) with good results. The Dunne runoff $R_1(y)$, which is a function of vertical depth y, can be expressed by

$$R_1(y) = \begin{cases} y - \dfrac{i_{\rm m}}{b+1}\left[\left(1-\dfrac{i_0}{i_{\rm m}}\right)^{b+1} - \left(1-\dfrac{i_0+y}{i_{\rm m}}\right)^{b+1}\right] , & 0 \leqslant y \leqslant i_{\rm m} - i_0 , \\ R_1(y)|_{y=i_{\rm m}-i_0} + y - (i_{\rm m}-i_0) , & i_{\rm m} - i_0 < y \leqslant P , \end{cases} \tag{2}$$

and the Horton runoff $R_2(y)$ can be represented in the following form:

$$R_2(y) = \begin{cases} P - R_1(y) - f_{\rm mm}\Delta t\left[1 - \left(\dfrac{P-R_1(y)}{f_{\rm m}\Delta t}\right)^{B+1}\right] , & \dfrac{P-R_1(y)}{f_{\rm m}\Delta t} \leqslant 1 , \\ P - R_1(y) - f_{\rm mm}\Delta t, & \dfrac{P-R_1(y)}{f_{\rm m}\Delta t} \geqslant 1 , \end{cases} \tag{3}$$

where i_0 and $i_{\rm m}$ are the initial infiltration capacity and maximum infiltration capacity, b is the shape parameter of the infiltration capacity, P represents the amount of precipitation over a time step Δt, $f_{\rm mm}$ is the average infiltration capacity over initially unsaturated area which can be derived by Philip infiltration formula, $f_{\rm m}$ is the maximum potential infiltration rate, and B is the potential infiltration rate shape parameter. The original surface runoff in the land surface model BATS version 1e (Biosphere-Atmosphere Transfer Scheme, and see also section 2.4) is simply parameterized as a function of soil moisture and net water to the surface.

Subsurface runoff parameterization is regarded as an exponential function of water table depth (Niu et al., 2005), i.e.,

$$R_{\rm sb} = R_{\rm sb,max} e^{-f z_\nabla} , \tag{4}$$

where $R_{\rm sb,max}$ is the maximum subsurface runoff for a grid cell with a zero mean water-table depth, here given a value of 1.0×10^{-4} mm s^{-1}, which is consistent with the maximum subsurface runoff in the BATS model; z_∇ is the grid cell mean water table depth; and f is a decay factor determined through a sensitivity analysis, here given a value of 2.0, following Niu et al. (2005) and the parameterization in CLM2.0.

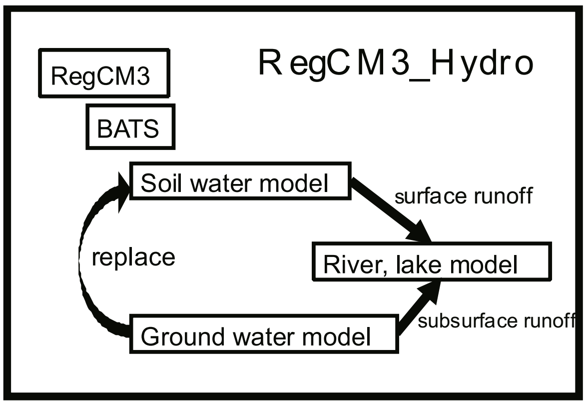

Fig. 1. Schematic diagram of groundwater model coupled with regional climate model RegCM3.

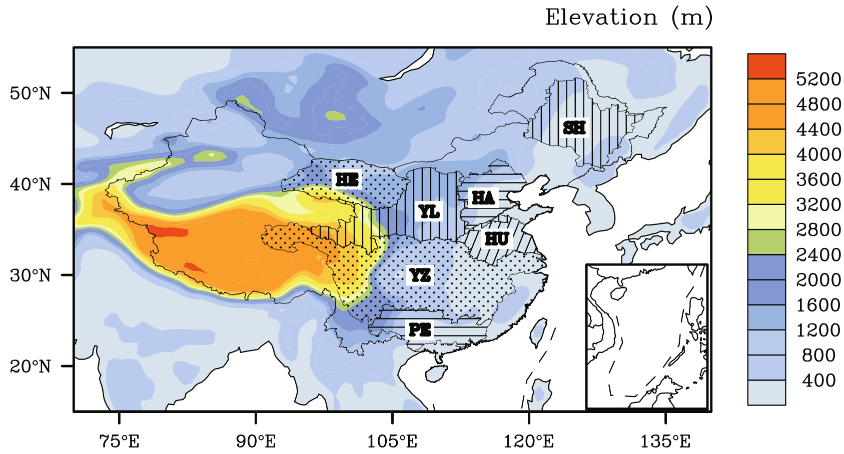

Fig. 2. Study domain and distribution of seven river basins in China: Yangtze River Basin (YZ), Haihe River Basin (HA), Heihe River Basin (HE), Huaihe River Basin (HU), Yellow River Basin (YL), Songhua River Basin (SH), and Pearl River Basin (PE).

2.4 *Model development*

As shown in Fig. 1, the groundwater model and surface and subsurface runoff parameterizations were incorporated into the BATS1e. A regional climate model was then implemented as the new coupled model RegCM3_Hydro, based on RegCM3 but with groundwater and new surface/subsurface runoff schemes added (Yuan, 2008).

2.5 *Setup of numerical experiments*

In this study, the regional climate models RegCM3 and RegCM3_Hydro were used to simulate the regional climate over east Asia (Fig. 2), centered on 36°N, 102°E, with a horizontal resolution of 60 km, 120×90 grid points, and 18 vertical layers. The model top is at 50 mbar. Simulations were performed in time steps of 200 s for atmospheric integration and 1800 s for land surface integration. The initial and boundary conditions driving the regional climate model were extracted from the European Centre for Medium-Range Weather Forecasts (ECMWF) 40-year reanalysis data sets (ERA-40). The data source for oceanic surface forcing was the Global Sea Ice and Sea Surface Temperature (GISST) 1° monthly gridded data provided

Table 1. Statistics of mean precipitation and 2-m mean temperature simulated by RegCM3 and RegCM3_Hydro.

	Precipitation						2 m temperature					
	ME[a] (mm d^{-1})		RMSE[b] (mm d^{-1})		CC[c]		ME (°C)		RMSE (°C)		CC	
	CTL	HYD	CTL	HYD	CTL	HYD	CTL	HYD	CTL	HYD	CTL	HYD
YZ	0.34	0.24	1.10	1.11	0.50	0.50	−5.83	−5.25	6.58	6.15	0.94	0.94
HA	0.81	0.59	0.95	0.76	0.04	−0.11	−3.55	−2.75	3.87	3.17	0.90	0.90
HE	0.35	0.32	0.67	0.65	0.80	0.8	−4.29	−3.91	4.73	4.39	0.83	0.83
HU	−0.01	−0.21	0.20	0.29	0.90	0.92	−2.39	−1.51	2.44	1.60	0.80	0.79
YL	0.53	0.47	0.66	0.64	0.69	0.65	−4.49	−3.88	4.80	4.28	0.96	0.96
SH	1.10	0.99	1.11	1.00	0.88	0.89	−1.11	−0.85	1.50	1.26	0.87	0.88
PE	0.34	0.28	0.62	0.57	0.80	0.82	−5.46	−4.94	5.51	4.99	0.95	0.95

[a] Systematic error: ME $= \frac{1}{N}\sum_{n=1}^{N}(x_{\mathrm{m},n}-x_{\mathrm{o},n})$, where $x_{\mathrm{m},n}$ and $x_{\mathrm{o},n}$ are the simulated and observed precipitation or temperature of grid n, respectively, and N is the grid number of the basin. [b] Root mean square error: RMSE $=\sqrt{\frac{1}{N}\sum_{n=1}^{N}(x_{\mathrm{m},n}-x_{\mathrm{o},n})^2}$.

[c] Spatial correlation coefficient: CC $= \dfrac{\sum_{n=1}^{N}(x_{\mathrm{m},n}-\overline{x_{\mathrm{m}}})(x_{\mathrm{o},n}-\overline{x_{\mathrm{o}}})}{\sqrt{\sum_{n=1}^{N}(x_{\mathrm{m},n}-\overline{x_{\mathrm{m}}})^2\cdot\sum_{n=1}^{N}(x_{\mathrm{o},n}-\overline{x_{\mathrm{o}}})^2}}$.

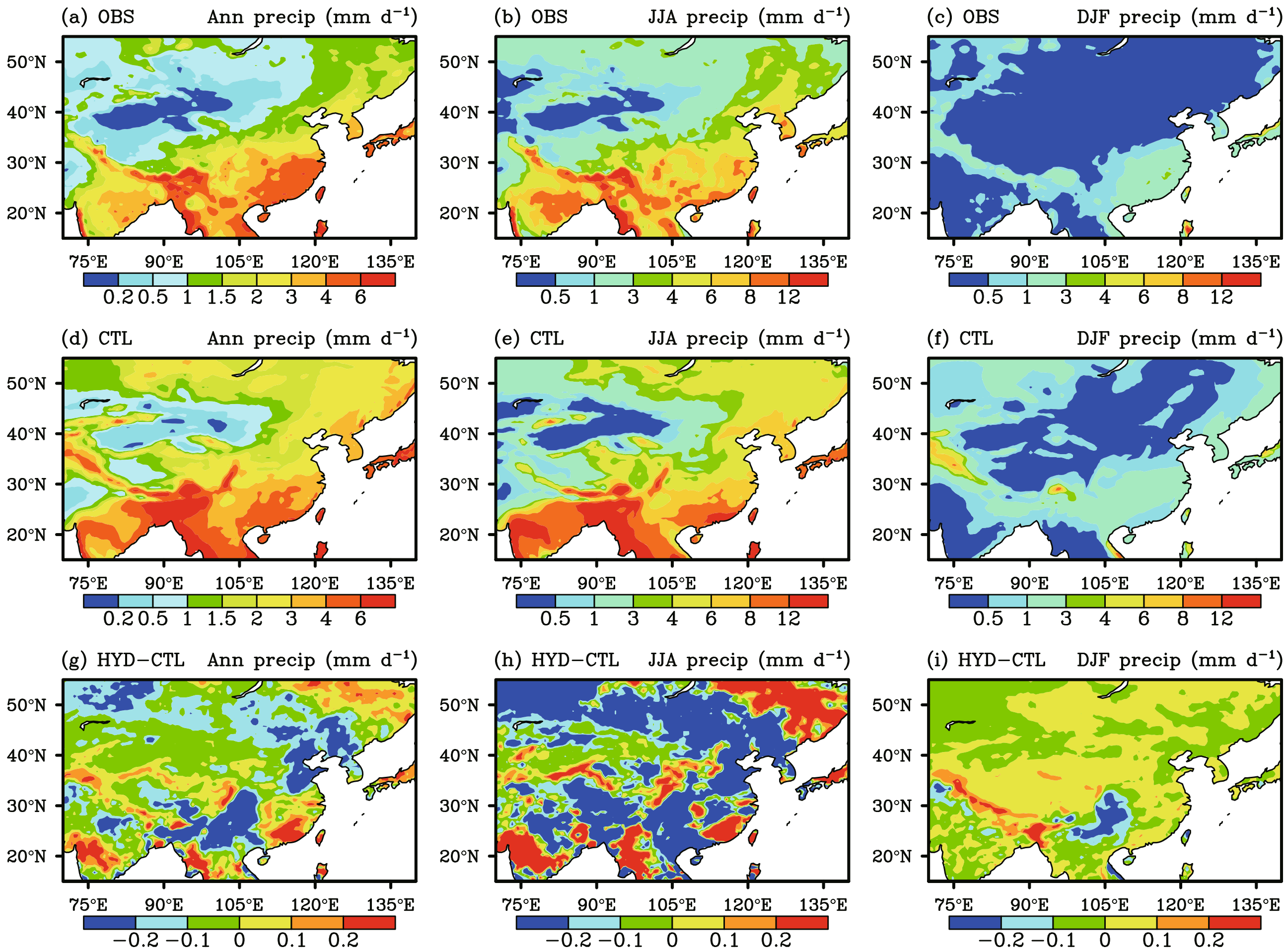

Fig. 3. Spatial distributions of annual and seasonal (JJA, DJF) mean precipitation (mm d-1) for observation data (a–c), RegCM3 (CTL) simulation (d–f), and the differences between RegCM3 and RegCM3_Hydro (HYD) simulation results (g–i).

by the Met Office Hadley Centre, Exeter, UK. The Grell scheme of cumulus convection (Grell, 1993) was adopted, with Fritsch and Chappell closure (Fritsch and Chappell, 1980). An initial water table depth of 3 m was chosen as the soil depth for RegCM3 simulations. The models were integrated for 45-year simulations for the period 1 September 1957–28 August 2002. The simulation results were analyzed for the period commencing 1 September 1982. The first 25 years of the simulations (1957–82) were omitted from the analysis, but were used as spin-up for groundwater activity. Finally, RegCM3 and RegCM3_Hydro outputs were interpolated to 0.5°×0.5°, and daily precipitation data sets with resolution 0.5°×0.5° during 1978–2003 from the Climate Prediction Center (CPC) Unified Gauge-Based Analysis (Xie et al., 2007) and CRU (Climate Research Unit) monthly temperature data sets with resolution 0.5°×0.5° from 1982 to 2002 (New et al., 2000) were used for model evaluation.

3. Results

3.1 *Precipitation and temperature*

Precipitation and temperature are the most commonly studied meteorological factors in climate research. Figure 3 shows the spatial distribution of annual and seasonal (JJA, DJF) mean precipitation (mm) based on observation data and RegCM3 simulations, and the disparities between RegCM3 and RegCM3_Hydro results for the period 1 September 1982 to 28 August 2002 for the East Asian monsoon area. Both models captured the overall spatial pattern of precipitation–that is, southern flood and northern drought, with most of the precipitation occurring during summer (JJA) in southeastern China (Figs. 3a–b, d–e, g–h). Compared with the RegCM3 simulation, results from the RegCM3_Hydro simulation incorporating the amended hydrological processes showed less annual and JJA precipitation and a reduction of positive biases in six of seven river basins (0.22 mm d^{-1} in the HA river basin), the exception being the HU river basin in the eastern part of China, where the negative bias was increased by 0.20 mm d^{-1} (Fig. 3g and Table 1). They also showed a smaller negative bias for simulated precipitation in the PE and lower YZ basins but an increased positive bias in the area north of the Heilongjiang River (Fig. 3g). Because most areas in China are cold and dry in winter and hot and wet in summer, JJA precipitation contributes greatly to annual precipitation (Fig. 3). The systematic bias of JJA precipitation simulated by RegCM3_Hydro averaged over the whole area was reduced from 0.35 mm d^{-1} to 0.31 mm d^{-1}, and decreased by 0.06 mm d^{-1} for annual precipitation.

Figure 4 shows a comparison between the observed and simulated spatial distributions of annual and seasonal (JJA, DJF) mean temperature at 2 m by both the RegCM3 and RegCM3_Hydro models. While they both simulated the observations well, they both underestimated the temperature over the whole studied area (Figs. 4a, d, and g). The value given by RegCM3_Hydro was higher than that of RegCM3 in most areas, thus reducing the negative bias from RegCM3 by more than 0.6°C, especially in the HA and HU river basins where negative biases were reduced by 0.80°C and 0.88°C, respectively (Fig. 4g and Table 1). In general, RegCM3_Hydro reduced the systematic bias of the mean annual temperature at 2 m by 0.25°C. The JJA temperature at 2 m simulated by RegCM3_Hydro was closer to observed temperature than RegCM3 in the northeastern area, but no clear improvement was found for the DJF temperatures at 2 m (Figs. 4h and i). The systematic negative bias of the simulated temperatures at 2 m averaged over the whole area from RegCM3 was reduced from 3.35°C to 2.83°C for JJA, and from 1.23°C to 1.1°C for DJF.

Figures 5a–g show the observed and simulated annual cycle of precipitation (mm d^{-1}) in the seven

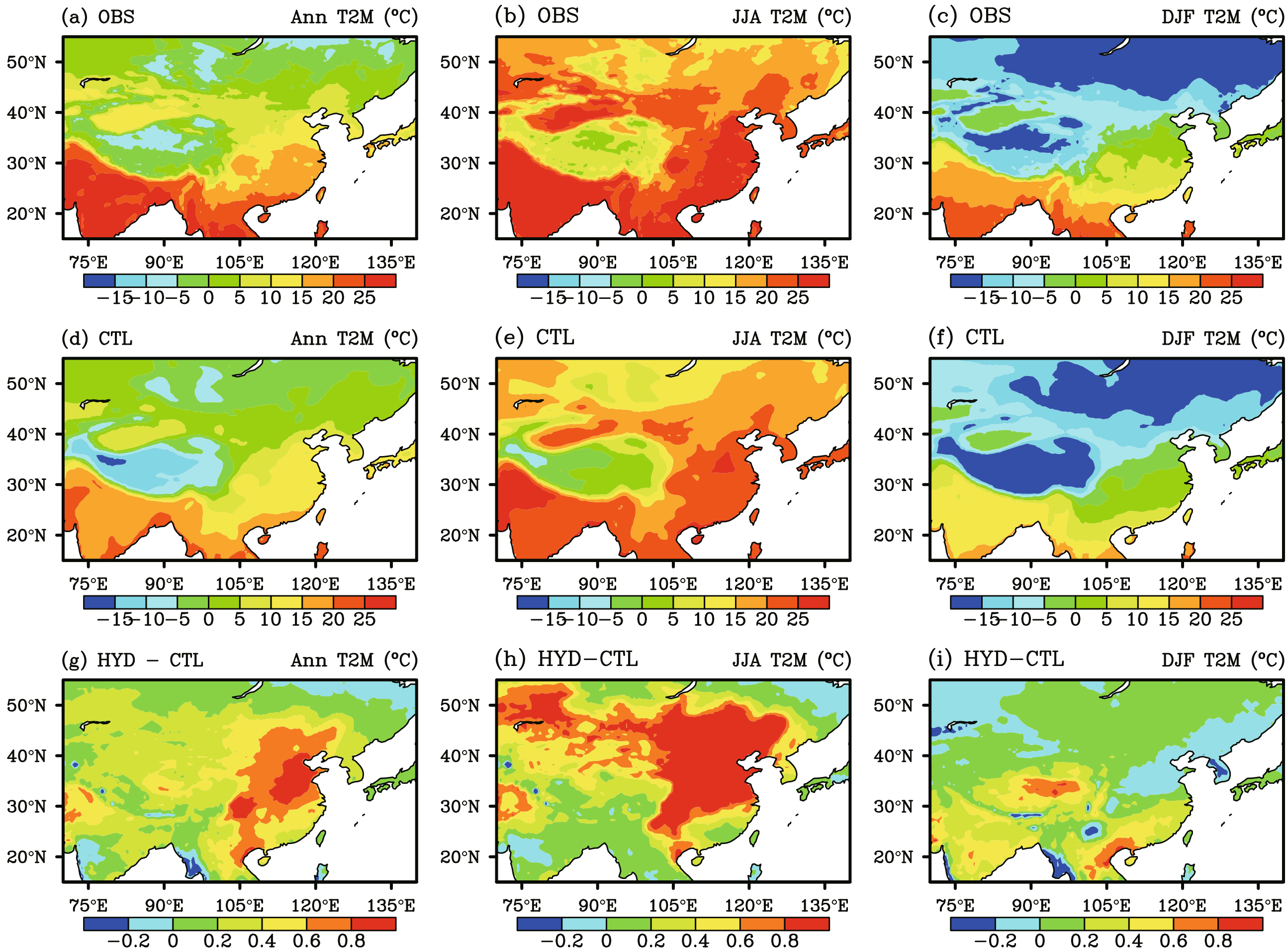

Fig. 4. The same as Fig. 3, but for 2-m temperature.

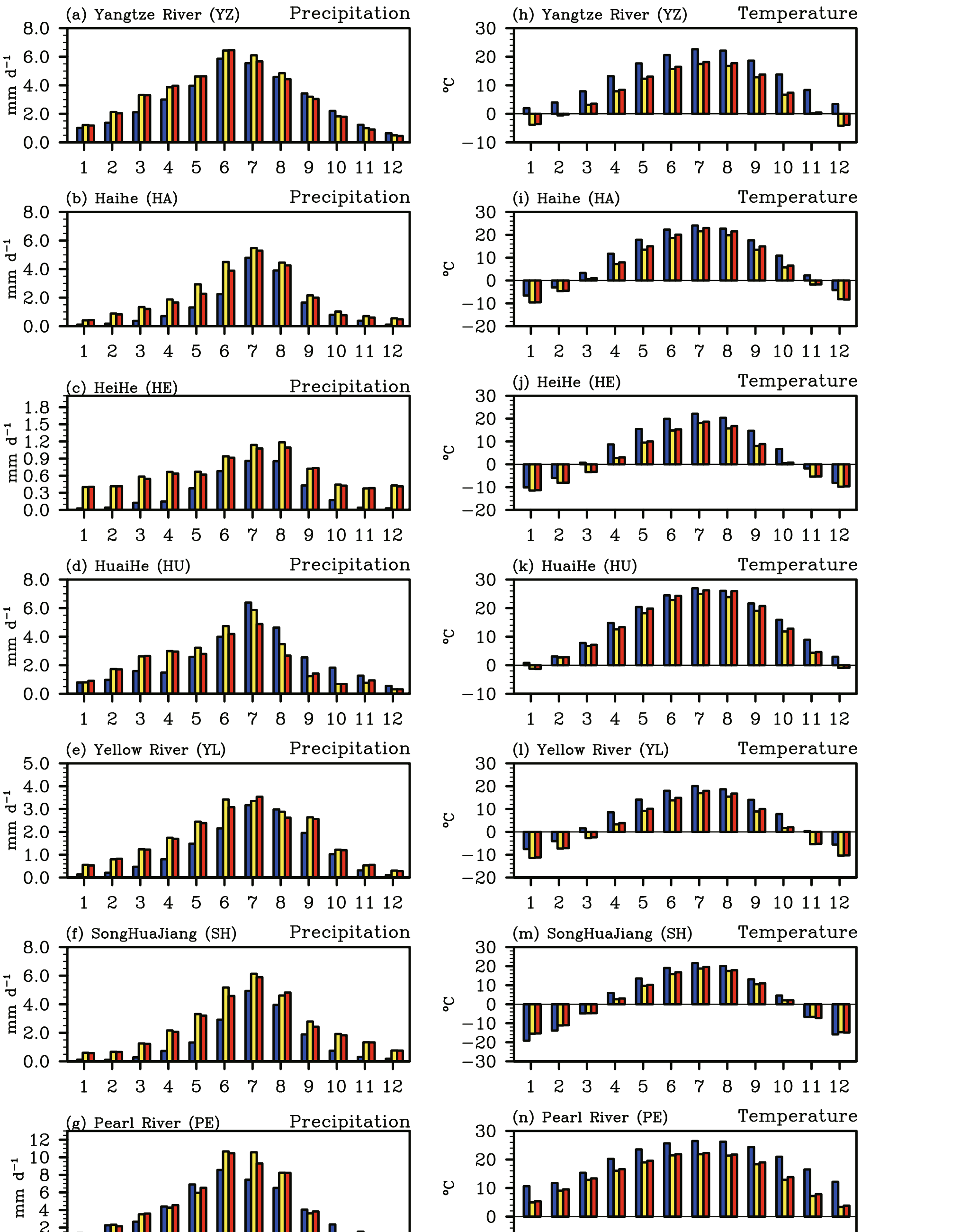

Fig. 5. Simulated and observed monthly mean precipitation (mm d^{-1}) and temperature (°C) averaged over seven river basins.

river basins. Both RegCM3 and RegCM3_Hydro captured the seasonal cycle and the differences among the basins. RegCM3_Hydro reduced the wetter biases of the summer monthly mean precipitation in the HA, HE, PE river basins, and increased the drier biases in the HU river basin. In general, compared with observed precipitation and the RegCM3 simulation, the RegCM3_Hydro simulation recorded lower JJA precipitation biases in six of the seven river basins of China in the present study, the exception being the HU basin in northwestern China. Figures 5h–n show the seasonal cycle of observed and simulated monthly mean temperatures at 2 m in the seven river basins. As in the precipitation results, the seasonal cycle and differences of temperature in the different basins were well captured by both the RegCM3 control and RegCM3_Hydro.

The latter simulations demonstrably reduced the negative bias of summer temperature over all of the studied river basins. The summer temperatures simulated by RegCM3_Hydro also closely matched observed temperatures in the HU river basin.

3.2 *Land surface conditions*

The water table and surface/subsurface runoff influence the soil moisture content through affecting the fluxes of the upper and lower boundaries of the soil column. Figure 6 shows the mean simulated annual top layer of soil moisture, root layer soil moisture, latent heat flux, sensible heat flux, surface runoff, and water-table depth for the RegCM3 control run and/or RegCM3_Hydro. Table 2 shows the annual and JJA differences in land surface water and energy variables in the seven river basins from 1 September 1982 to 28 August 2002. Figure 6 and Table 2 show that the soil moisture content of both the top layer and the root layer simulated by RegCM3_Hydro was drier than soil moisture content generated by RegCM3 (see also Figs. 7a–n).

This result indicates that surface evaporation was reduced, and therefore lower evapotranspiration took place, in all the river basins. In the HU river basin in particular, the simulation indicated that JJA evapotranspiration was reduced by 1.18 mm d^{-1} (Table 2). Lower evapotranspiration was simulated to cause a reduction in JJA latent heat flux by 16.74 W m^{-2} (YZ), 29.87 W m^{-2} (HA), 3.27 W m^{-2} (HE), 34.27 W m^{-2} (HU), 17.05 W m^{-2} (YL), 8.38 W m^{-2} (SH), and 6.43 W m^{-2} (PE) , and therefore a warmer surface was obtained for those areas. Differences in surface water and other variables influence the total precipitation changes by affecting the boundary layer. Due to implementation of surface runoff scheme, RegCM3_Hydro increased JJA surface runoff by 0.84 mm d^{-1} (YZ), 0.71 mm d^{-1} (HA), 0.22 mm d^{-1} (HE), 0.55 mm d^{-1} (HU), 0.55 mm d^{-1} (YL), 0.75 mm d^{-1} (SH), and 1.10 mm d^{-1} (PE), and annual surface runoff by 0.48 mm d^{-1} (YZ), 0.31 mm d^{-1} (HA), 0.11 mm d^{-1} (HE), 0.37 mm d^{-1} (HU), 0.29 mm d^{-1} (YL), 0.29 mm d^{-1} (SH), and 0.62 mm d^{-1} (PE). The amplitude of total runoff simulated by RegCM3_Hydro was smaller than of RegCM3 (Figs. 7o–u).

Figure 8 shows the simulated monthly mean land surface variables over the seven river basins. Compared with RegCM3, the RegCM3_Hydro suggested a drier top layer and root layer soil moisture, lower latent heat flux, higher sensible heat flux, and more surface runoff during the summer months in all except the HE basin, for which no obvious differences were found.

RegCM3_Hydro also simulated the spatial distri-

Table2. Annual and JJA mean differences (RegCM3_Hydro minus RegCM3) in land surface water and energy variables averaged over seven river basins.

Variables	YZ		HA		HE		HU		YL		SH		PE	
	ANN	JJA	ANN	JJA	ANN	JJA	ANN	JJA	ANN	JJA	ANN	JJA	ANN	JJA
Differences in water variables														
Top layer soil moisture (mm mm^{-1})	−0.34	−0.58	−0.50	−1.03	−0.05	−0.11	−0.56	−1.18	−0.26	−0.59	−0.14	−0.29	−0.38	−0.22
Root layer soil moisture (mm mm^{-1})	−0.05	−0.05	−0.04	−0.05	−0.01	−0.01	−0.02	−0.04	−0.04	−0.04	−0.06	−0.06	−0.05	−0.05
Surface runoff (mm d^{-1})	0.48	0.84	0.31	0.71	0.11	0.22	0.37	0.55	0.29	0.55	0.29	0.75	0.62	1.10
Evapotranspiration (mm d^{-1})	−0.34	−0.58	−0.50	−1.03	−0.05	−0.11	−0.56	−1.18	−0.26	−0.59	−0.14	−0.29	−0.38	−0.22
Total precipitation (mm d^{-1})	−0.10	−0.28	−0.22	−0.44	−0.03	−0.07	−0.20	−0.78	−0.05	−0.15	−0.11	−0.16	−0.06	−0.53
Differences in energy variables														
2 m mean temperature (°C)	0.58	0.83	0.80	1.67	0.38	0.71	0.88	1.69	0.60	1.17	0.26	0.75	0.52	0.43
Net absorbed shortwave (W m^{-2})	3.85	5.43	2.76	5.83	1.12	1.43	3.35	10.24	1.33	2.42	4.49	10.73	3.99	6.25
Net longwave (W m^{-2})	5.13	7.25	6.15	12.51	1.42	2.67	5.96	13.49	3.38	7.12	4.34	8.48	5.53	4.78
Latent heat flux (W m^{-2})	−9.97	−16.74	−14.49	−29.87	−1.32	−3.27	−16.27	−34.27	−7.66	−17.05	−3.92	−8.38	−11.08	−6.43
Sensible heat flux (W m^{-2})	8.75	15.14	11.05	22.78	1.15	1.91	13.43	30.42	5.56	12.2	4.68	10.89	9.35	8.02

YZ: Yangtze River Basin, HA: Haihe River Basin, HE: Heihe River Basin, HU: Huaihe River Basin, YL: Yellow River Basin, SH: Songhua River Basin, PE: Pearl River Basin.

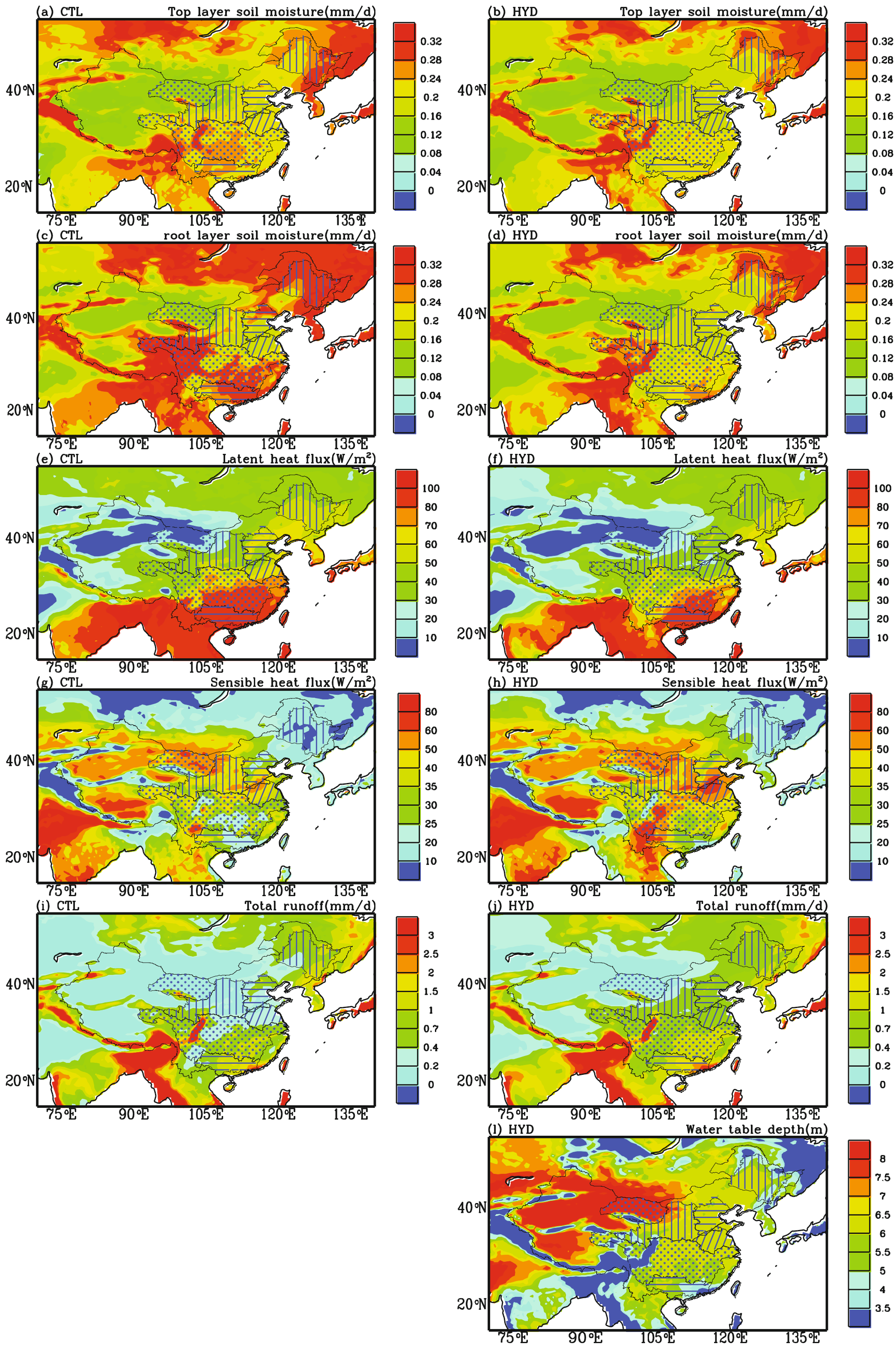

Fig. 6. Simulated annual mean top layer soil moisture (a, b), root layer soil moisture (c, d), latent heat flux (e, f), sensible heat flux (g, h), surface runoff (i, j), and water table depth (l) by RegCM3 and/or RegCM3_Hydro.

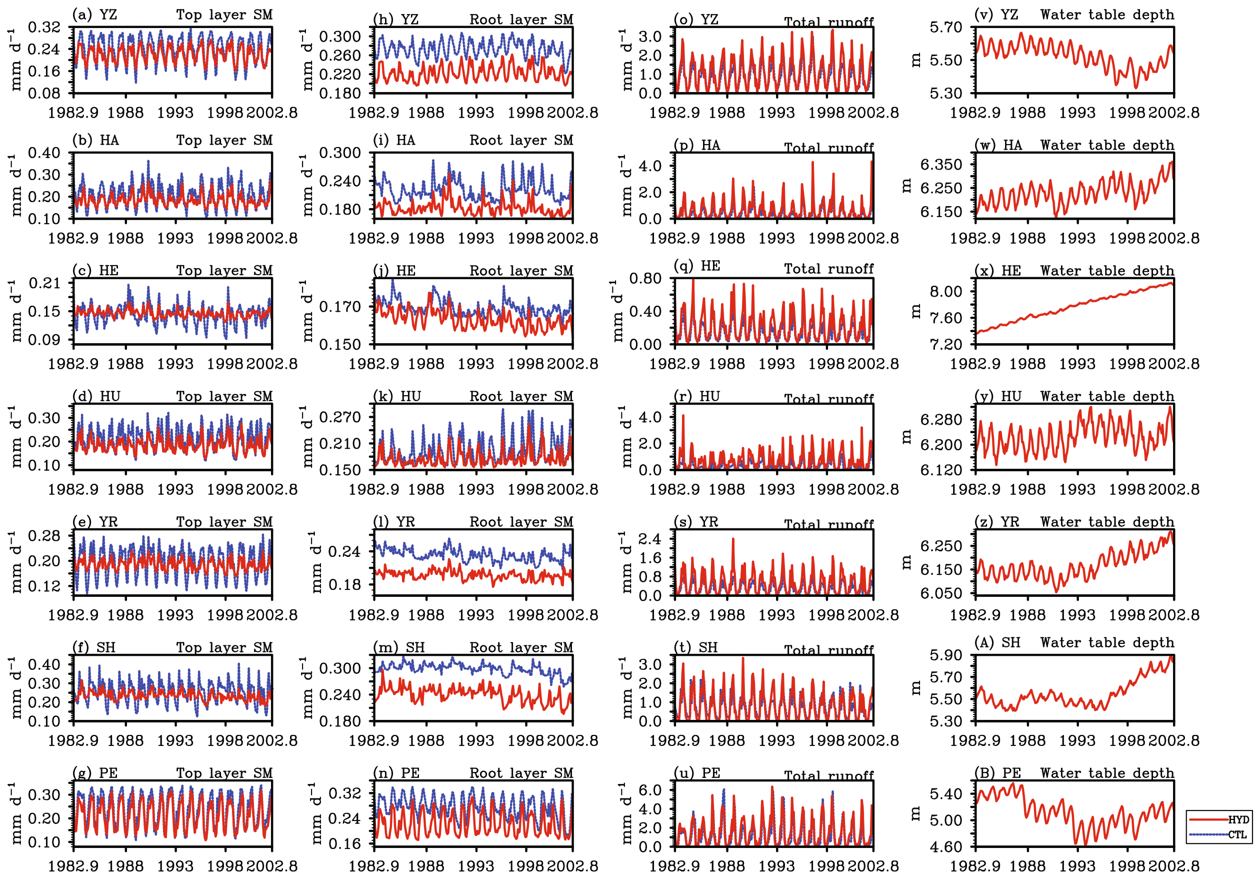

Fig. 7. Simulated time series of top layer and root layer soil moisture (a–g, h–n), total runoff (o–u) and water table depth (v–B) averaged over seven river basins in China.

bution of water-table depth in the study area (Fig. 6l), indicating shallow water table in southern China and deep water table in the northern and northwestern China. Obvious seasonal variation of water-table depth was also captured by RegCM3_Hydro in those areas with a shallow water table, such as the lower reaches of the YZ river basin (Figs. 8a.6–g.6). The deepest water table occurred in autumn and the shallowest occurred in spring.

4. Conclusion and discussion

In this study we augmented the regional climate model RegCM3 with a groundwater model and surface/subsurface runoff parameterizations. Results of 20-year simulations by the RegCM3 and the newly developed RegCM3_Hydro numerical models show that both models captured the spatial pattern of precipitation reasonably, with most of the rain falling during the summer months (JJA) in the monsoon area of China. Using the developed groundwater process and runoff schemes, the bias of the simulated mean annual precipitation produced by the RegCM3_Hydro model was reduced in six of seven river basins (0.22 mm d^{-1} in the HA river basin), the exception being the HU river basin in the eastern part of China, where the negative bias was increased by 0.20 mm d^{-1}. The temperature simulated by the RegCM3_Hydro model was higher than that simulated by RegCM3 in most areas. RegCM3_Hydro reduced the negative bias in annual temperature, especially in HA and HU river basins, where the reductions were 0.80°C and 0.88°C, respectively. In general, the systematic bias for mean annual precipitation, as simulated by RegCM3_Hydro, was reduced by 0.06 mm d^{-1}, and the systematic bias for temperature at 2 m was reduced by 0.25°C. RegCM3_Hydro also captured the spatial distribution and seasonal changes of water-table depth in the basins, indicating drier upper soil layer and root layer, less latent heat flux, more sensible heat flux and more surface runoff in the seven basins.

This results of this study showed dryer conditions (both top layer soil moisture and root layer soil moisture), whereas the results of Yuan et al. (2008) showed wetter soil moisture. This difference is mainly due to the new surface runoff adopted here, which caused

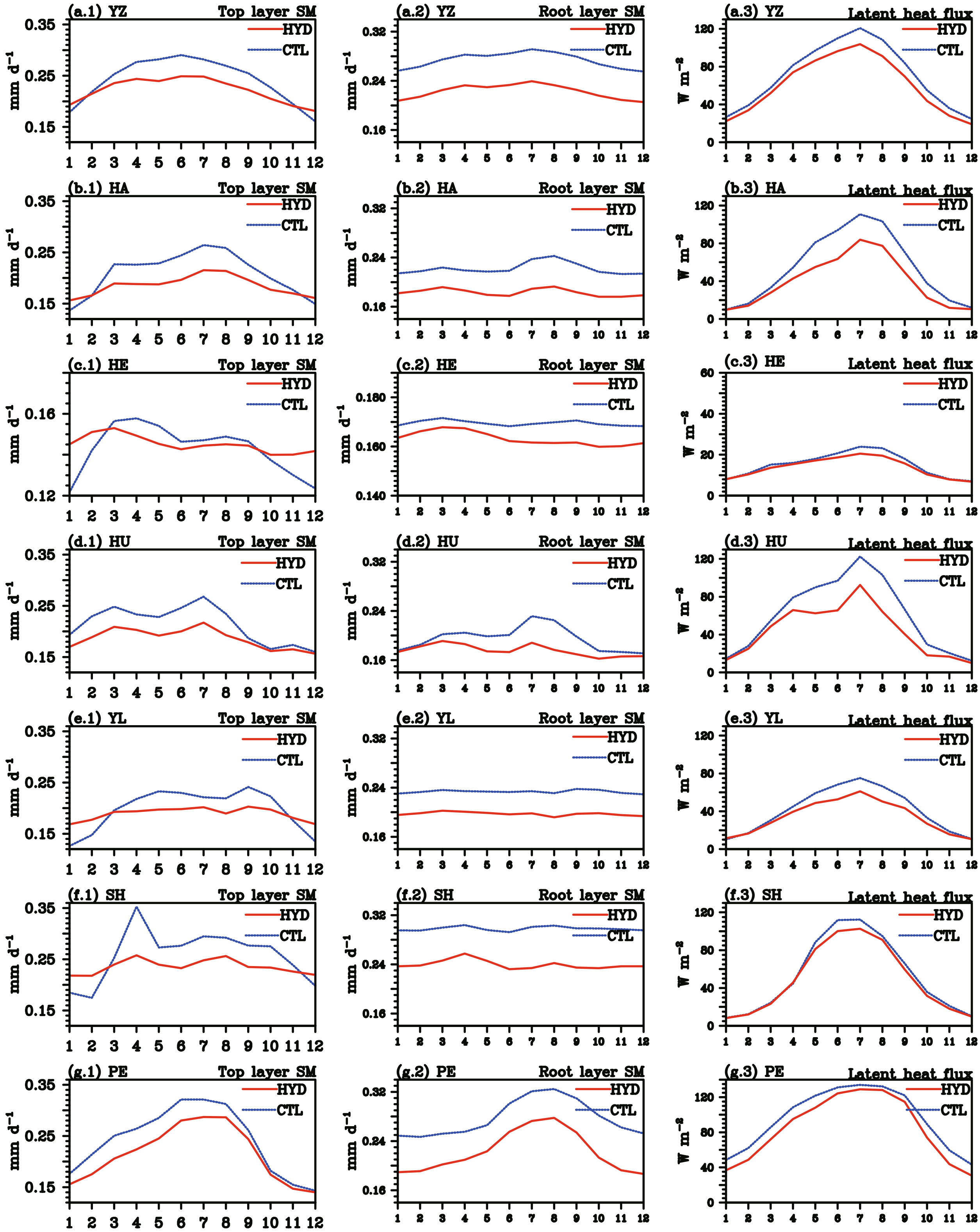

Fig. 8. Simulated monthly mean land surface variables averaged overseven river basins: top layer soil moisture (a.1–g.1), root layer soil moisture (a.2–g.2), latent heat flux (a.3–g.3), sensible heat flux (a.4–g.4), surface runoff (a.5–g.5) and water table depth (a.6–g.6).

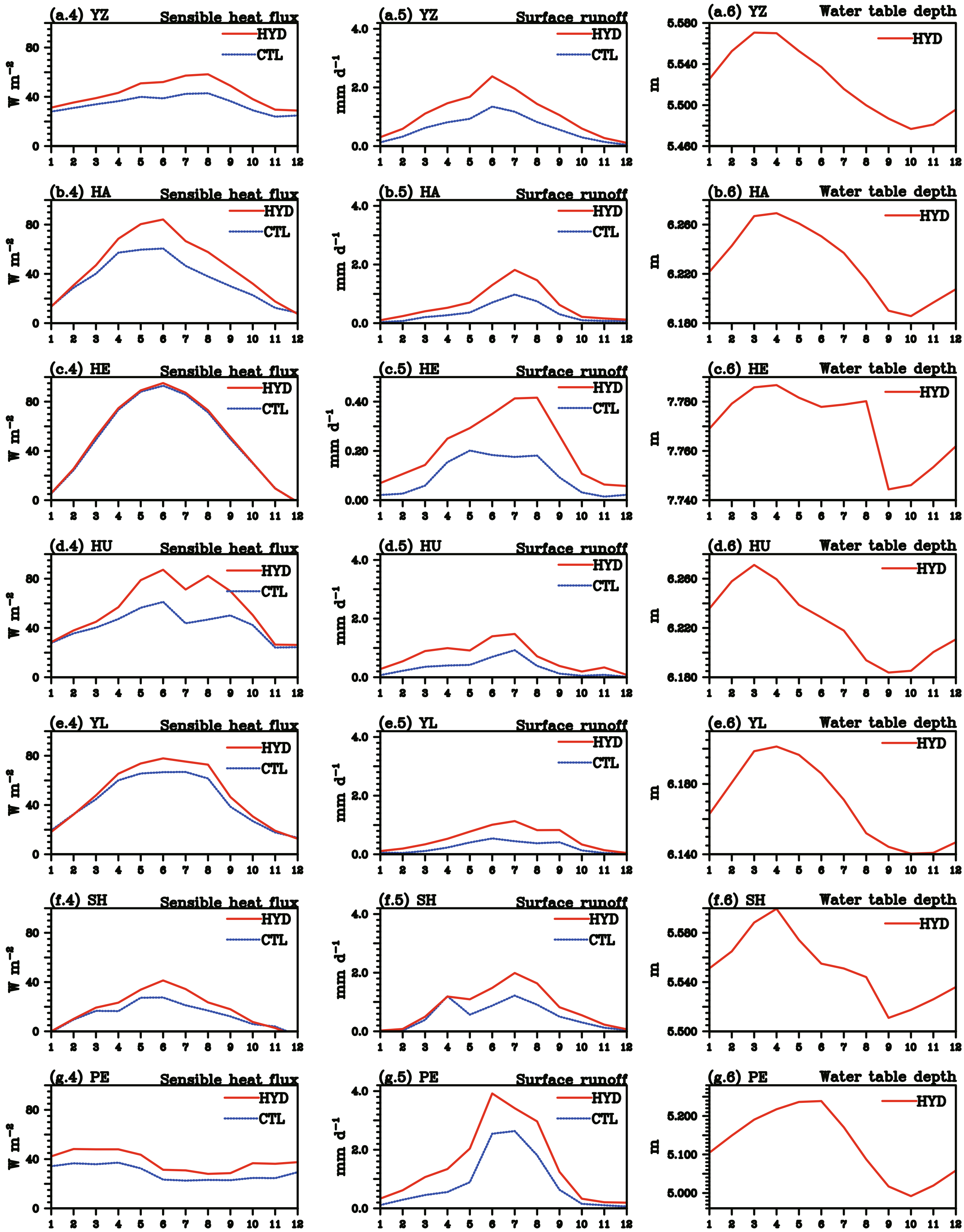

Fig. 8. (Continued).

more surface runoff (as showed in Fig. 8) in all seven river basins of China and outweighed groundwater, thus leading to dryer soil moisture. Due to the lack of a detailed groundwater description that includes lateral flow, the challenge for land surface and climate system modeling continues to be the development of a more accurate groundwater model that includes lateral flow data.

Acknowledgements. This work was supported by the National Basic Research Program of China (Grant Nos. 2009CB421407 and 2010CB428403), the National Natural Science Foundation of China (Grant No. 91125016), the Chinese Academy of Sciences Strategic Priority Research Program (Grant No. XDA05110102), and the National High Technology Research and Development Program of China (Grant No. 2010AA012301).

REFERENCES

Beven, K., and M. Kirkby, 1979: A physically based, variable contributing area model of basin hydrology/Un modèle à base physique de zone d'appel variable de l'hydrologie du bassin versant. *Hydrological Sciences Bulletin*, **24**(1), 43–69.

Di, Z., Z. Xie, X. Yuan, X. Tian, Z. Luo, and Y. Chen, 2011: Prediction of water table depths under soil water-groundwater interaction and stream water conveyance. *Sci. China* (*D*), **54**(3), 420–430, doi: 10.1007/s11430-010-4050-8.

Dickinson, R., A. Henderson-Sellers, and D. M. Kennedy, 1993: Biosphere-Atmosphere Transfer Scheme (BATS) version le as coupled to the NCAR Community Climate Model. NCAR Tech. Note NCAR=TN-3874STR, 72pp.

Fritsch, J. M., and C. F. Chappell, 1980: Numerical prediction of convectively driven mesoscale pressure systems .1. Convective parameterization. *J. Atmos. Sci.*, **37**(8), 1722–1733.

Gao, X. J., Y. Shi, and F. Giorgi, 2011: A high resolution simulation of climate change over China. *Sci. China* (*D*), **54**(3), 462–472 doi: 10.1007/s11430-010-4035-7.

Gao, X. J., Y. Shi, D. F. Zhang, and F. Giorgi, 2012: Climate change in China in the 21st century as simulated by a high resolution regional climate model. *Chinese Science Bulletin,* **57**(10), 1188–1195, doi: 10.1007/s11434-011-4935-8.

Giorgi, F., M. R. Marinucci, and G. T. Bates, 1993a: Development of a 2nd-Generation Regional Climate Model (Regcm2). 1. Boundary-layer and radiative-transfer processes. *Mon. Wea. Rev.*, **121**(10), 2794–2813.

Giorgi, F., M. R. Marinucci, G. T. Bates, and G. Decanio, 1993b: Development of a 2nd-Generation Regional Climate Model (Regcm2). 2. Convective processes and assimilation of lateral boundary-conditions. *Mon. Wea. Rev.*, **121**(10), 2814–2832.

Giorgi, F., R. Francisco, and J. Pal, 2003: Effects of a subgrid-scale topography and land use scheme on the simulation of surface climate and hydrology. Part I: Effects of temperature and water vapor disaggregation. *Journal of Hydrometeorology*, **4**(2), 317–333.

Grell, G. A., 1993: Prognostic evaluation of assumptions used by cumulus parameterizations. *Mon. Wea. Rev.*, **121**(3), 764–787.

Grell, G. A., J. Dudhia, and D. R. Stauffer, 1994: A description of the fifth generation Penn State/NCAR Mesoscale Model (MM5), NCAR Tech. Note TN-398+STR, 121pp.

Henriksen, H. J., L. Troldborg, P. Nyegaard, T. O. Sonnenborg, J. C. Refsgaard, and B. Madsen, 2003: Methodology for construction, calibration and validation of a national hydrological model for Denmark. *J. Hydrol.*, **280**(1–4), 52–71.

Holtslag, A. A. M., and B. A. Boville, 1993: Local versus nonlocal boundary-layer diffusion in a global climate model. *J. Climate*, **6**(10), 1825–1842.

Holtslag, A. A. M., E. I. F. Debruijn, and H. L. Pan, 1990: A high-resolution air-mass transformation model for short-range weather forecasting. *Mon. Wea. Rev.*, **118**(8), 1561–1575.

Hu, Y., Y. Ding, and F. Liao, 2010: An improvement on summer regional climate simulation over East China: Importance of data assimilation of soil moisture. *Chinese Science Bulletin*, **55**(9), 865–871.

Im, E. S., E. Coppola, F. Giorgi, and X. Bi, 2010: Validation of a high-resolution regional climate model for the Alpine region and effects of a subgrid-scale topography and land use representation. *J. Climate*, **23**(7), 1854–1873.

Kiehl, J. T., J. J. Hack, G. B. Bonan, B. A. Boville, B. P. Briegleb, D. L. Williamson, and P. J. Rasch, 1996: Description of the NCAR Community Climate Model (CCM3). NCAR Tech. Rep. TN-420+STR, 152pp.

Liang, X., 2003: A new parameterization for surface and groundwater interactions and its impact on water budgets with the variable infiltration capacity (VIC) land surface model. *J. Geophys. Res.*, **108**(D16), 1–17.

Liang, X., and Z. H. Xie, 2001: A new surface runoff parameterization with subgrid-scale soil heterogeneity for land surface models. *Advances in Water Resources*, **24**(9–10), 1173–1193.

Liang, X., Z. Xie, and M. Huang, 2003: A new parameterization for surface and groundwater interactions and its impact on water budgets with the variable infiltration capacity (VIC) land surface model. *J. Geophys. Res.*, **108**(D16), 1–17.

Maxwell, R. M., and S. J. Kollet, 2008: Interdependence of groundwater dynamics and land-energy feedbacks under climate change. *Nature Geoscience*, **1**(10), 665–669.

New, M., M. Hulme, and P. Jones, 2000: Representing twentieth-century space-time climate variability. Part II: Development of 1901–96 monthly grids of terrestrial surface climate. *J. Climate*, **13**(13), 2217–2238.

Niu, G., Z. Yang, R. Dickinson, and L. Gulden, 2005: A simple TOPMODEL-based runoff parameterization (SIMTOP) for use in global climate models. *J. Geophys. Res*, **110**, D21106, doi: 10.1029/2005JD006111.

Niu, G. Y., Z. L. Yang, R. E. Dickinson, L. E. Gulden, and H. Su, 2007: Development of a simple groundwater model for use in climate models and evaluation with Gravity Recovery and Climate Experiment data. *J. Geophys. Res.*, **112**, D07103, doi: 10.1029/2006JD007522.

Pal, J. S., E. E. Small, and E. A. B. Eltahir, 2000: Simulation of regional-scale water and energy budgets: Representation of subgrid cloud and precipitation processes within RegCM. *J. Geophys. Res.*, **105**(D24), 29579–29594.

Pal, J. S., and Coauthors, 2007: Regional climate modeling for the developing world—The ICTP RegCM3 and RegCNET. *Bull. Amer. Meteor. Soc.*, **88**(9), 1395–1409.

Sivapalan, M., K. Beven, and E. Wood, 1987: On hydrologic similarity 2. A scaled model of storm runoff production. *Water Resour. Res.*, **23**(12), 2266–2278.

Sophocleous, M., and S. P. Perkins, 2000: Methodology and application of combined watershed and groundwater models in Kansas. *J. Hydrol.*, **236**(3–4), 185–201.

Sophocleous, M. A., J. K. Koelliker, R. S. Govindaraju, T. Birdie, S. R. Ramireddygari, and S. P. Perkins, 1999: Integrated numerical modeling for basin-wide water management: The case of the Rattlesnake Creek basin in south-central Kansas. *J. Hydrol.*, **214**(1–4), 179–196.

Steiner, A. L., J. S. Pal, F. Giorgi, R. E. Dickinson, and W. L. Chameides, 2005: The coupling of the Common Land Model (CLM0) to a regional climate model (RegCM). *Theor. Appl. Climatol.*, **82**, 225–243.

Syed, F., F. Giorgi, J. Pal, and K. Keay, 2010: Regional climate model simulation of winter climate over Central-Southwest Asia, with emphasis on NAO and ENSO effects. *Int J Climatol*, **30**(2), 220–235.

Sylla, M. B., E. Coppola, L. Mariotti, F. Giorgi, P. M. Ruti, A. Dell'Aquila, and X. Bi, 2010: Multiyear simulation of the African climate using a regional climate model (RegCM3) with the high resolution ERA-interim reanalysis. *Climate Dyn.*, **35**(1), 231–247.

Thrasher, B. L., and L. C. Sloan, 2010: Land cover influences on the regional climate of western North America during the early Eocene. *Global Planet Change*, **72**(1–2), 25–31.

Tian, X. J., Z. H. Xie, S. L. Zhang, and M. L. Liang, 2006: A subsurface runoff parameterization with water storage and recharge based on the Boussinesq-storage equation for a land surface model. *Sci. China (D)*, **49**(6), 622–631.

Van Den Hurk, B. J. J. M., and E. Van Meijgaard, 2010: Diagnosing land-atmosphere interaction from a regional climate model simulation over West Africa. *Journal of Hydrometeorology*, **11**(2), 467–481.

Xie, P., M. Chen, S. Yang, A. Yatagai, T. Hayasaka, Y. Fukushima, and C. Liu, 2007: A gauge-based analysis of daily precipitation over East Asia. *Journal of Hydrometeorology*, **8**, 607–626.

Xie, Z., and X. Yuan, 2010: Prediction of water table under stream-aquifer interactions over an arid region. *Hydrological Processes*, **24**, 160–169, doi: 10.1002/hyp.7434.

Xie, Z., Q. C. Zeng, Y. J. Dai, and B. Wang, 1998: Numerical simulation of an unsaturated flow equation. *Sci. China (D)*, **4**(14), 429–436.

Xie, Z., Q. C. Zeng, and Y. J. Dai, 1999: An unsaturated soil flow problem and its numerical simulation. *Adv. Atmos. Sci.*, **16**(2), 183–198.

Xie, Z., Z. Di, Z. Luo, and Q. Ma, 2012: A quasi-three-dimensional variably saturated groundwater flow model for climate modeling. *Journal of Hydrometeorology*, **13**, 27–46. doi: http://dx.doi.org/10.1175/JHM-D-10-05019.1.

Yang, H., and Z. Xie, 2003: A new method to dynamically simulate groundwater table in land surface model VIC. *Progress in Natural Science*, **13**(11), 819–825.

Yuan, X., 2008: Coupling of a regional climate model with a groundwater model. Phd thesis, Institute of Atmospheric Physics, Chinese Academy of Sciences, 170pp. (in Chinese)

Yuan, X., Z. H. Xie, J. Zheng, X. J. Tian, and Z. L. Yang, 2008: Effects of water table dynamics on regional climate: A case study over east Asian monsoon area. *J. Geophys. Res.*, **113**, D21112, doi: 10.1029/2008JD010180.

Zakey, A. S., F. Giorgi, and X. Bi, 2008: Modeling of sea salt in a regional climate model: Fluxes and radiative forcing. *J. Geophys. Res.*, **113**, D14221, doi: 10.1029/2007JD009209.

Zeng, X. B., M. Zhao, and R. E. Dickinson, 1998: Intercomparison of bulk aerodynamic algorithms for the computation of sea surface fluxes using TOGA COARE and TAO data. *J. Climate*, **11**(10), 2628–2644.

Zou, L. W., and T. J. Zhou, 2012: Development and evaluation of a regional ocean-atmosphere coupled model with focus on the western North Pacific summer monsoon simulation: Impacts of different atmospheric components. *Sci. China (D)*, **55**(5), 802–815.